Computational Studies on the Charge Transfer and Transport Properties of Molecular and Nano Interfaces

Synopsis of the Proposed Ph.D. Research Work

UNDER THE SUPERVISION OF

Prof. Dr. Pranab Sarkar

Prodyut Roy
Registration No.: VB-690 of 2011-12
Date of Registration: 29/11/2016
Department of Chemistry
Siksha-Bhavana
Visva-Bharati

Contents

1. Origin of the research problem
2. Objectives of our proposed research work
3. Methodology
4. Future Prospect
5. References

Origin of the research problem

The primary criteria for a chemical reaction to occur is the charge transfer between the reactants. This may be intramolecular or intermolecular, in the ground state or in the photochemically excited state. The rate of a chemical reaction explicitly depends on the rate of charge transfer. In presence of a catalyst the rate of the chemical reaction is improved by lowering the activation energy barrier of the chemical reaction thereby increasing the rate of charge transfer. The primary role of the catalyst is to assist the charge transfer processes through the involvement of one or more intermediate(s). Thus, in order to modulate the chemical reactivity one should have a concrete idea of charge transfer processes that occur at the catalyst-molecule interface. This is a vast and ever growing field of research where the nature of the catalyst changes from one form to other through the era of science. In the present days people are mainly involved for the development of more and more advanced nano catalysts which can efficiently perform their role in the synthesis of essential ingredients or to destroy environmentally hazardous materials.

Charge transport through molecular or nano interfaces, on the other hand, is also an evolving field of research that offers cheap and light conducting materials useful in nano technology. Engineering of such materials requires a concrete knowledge of electronic structure and inter-electronic coupling parameters at the nano interface. In the proposed thesis we would like to study the detailed electronic structure, energy level alignment, inter-electronic coupling, and mechanism of charge transfer and transport phenomena of some designed molecules and the interfaces with nano materials such as metal clusters or semiconductor surfaces.

Human civilization is getting modernized day-by-day with the use of various sophisticated machineries. To run these sophisticated machineries, a huge amount of energy is required. The main source of energy is the burning of fossil fuels like coal, natural gases etc. The burning of these fossil fuels releases huge amount of CO_2 in our environment, which is one of the major component of the greenhouse gases. Though there is other unconventional sources of energy like solar energy, hydro-electricity which do not evolve CO_2, they cannot fulfil the requirement of energy for running the modern civilization. So, the concentration of CO_2 in the environment is increasing day-by-day and consequently the threat of global warming is also increasing. There are natural systems for the consumption of CO_2 like photosynthesis. Green plants uses CO_2 for photosynthesis to convert solar energy into chemical energy and store it in the form of glucose and release O_2 in the environment. Glucose is the main source of energy for all the living creatures in the nature. In the mitochondria of the cells in the living bodies this glucose is burnt in presence of O_2 and releases energy which drives the life cycle of the living organisms. But due to modernization of the human society the requirement of infrastructural facilities is also increasing. For this infrastructural purpose deforestation is also increasing and the number of trees is getting drastically reduced. Due to this reason the balance between the amount of CO_2 produced and that fixed is getting disturbed. Other ways of CO_2 fixation include the deposition of carbonate salt in the ocean but through this way the amount of CO_2 fixation is very minute. Now the time has

reached, when we should think about the alternative way of fixation of carbon dioxide by developing systems for carrying out artificial fixation of CO_2. Several theoretical and experimental studies are being performed day-by-day to develop newer and efficient systems for the artificial conversion of carbon dioxide in the form of formic acid (HCOOH), CO, ethanol (EtOH) and other useful chemicals. Artificial fixation of CO_2 can be carried out by means of the two following processes: (a) photocatalysis using solar energy, i.e., ***artificial photosynthesis*** and (b) ***chemical reduction*** of carbon dioxide.

Artificial photosynthesis include photocatalytic splitting of water and the reduction of CO_2.[1-4] Carbon dioxide molecules are stable and chemically inert with a closed-shell electronic configuration, linear geometry, and $D_{\infty h}$ symmetry.[5, 6] The addition of a single electron causes a bending of the molecular structure because of repulsion between the newly acquired electron situated on the electrophilic carbon atom and the free electron pairs on the oxygen atoms. The loss of symmetry and the increased repulsion between these free electron pairs in the bent structure with a C_{2v} symmetry contribute to the high energy of the LUMO of CO_2 and thus the very low electron affinity of the molecule. The single-electron reduction of CO_2 to an anion radical $CO_2^{\bullet-}$ has, therefore, a strongly negative electrochemical potential of −1.9 V versus the normal hydrogen electrode (NHE).[7] In effect, virtually no semiconductor provides sufficient potential to transfer a single photogenerated electron to a free CO_2 molecule, thus making this step highly improbable.

$$CO_2 + e^- \rightarrow CO_2^{\bullet-} \qquad E^0_{red} = -1.9 \text{ V vs. NHE}$$

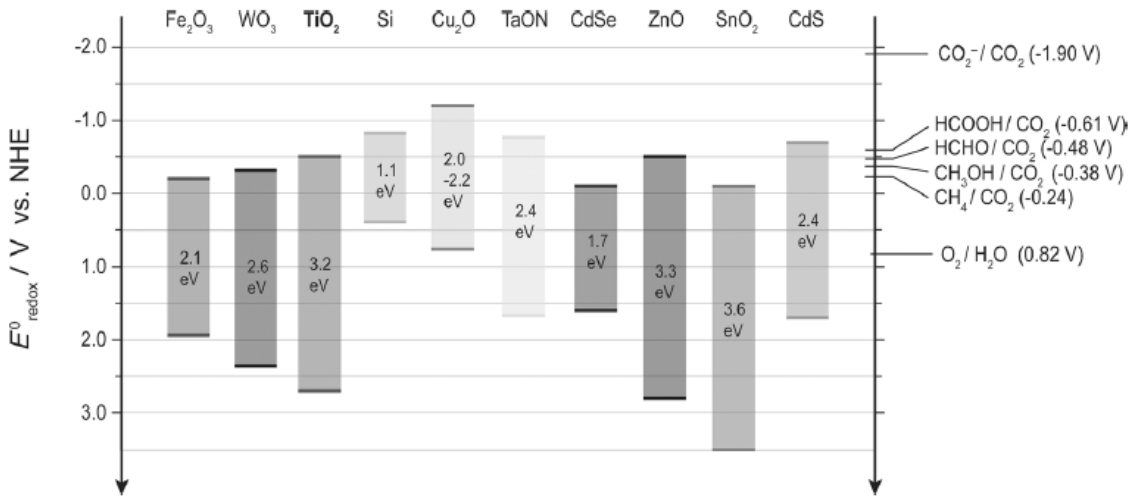

Figure 1: Schematic representation of conduction band, valence band potentials, and band gap energies of various semiconductor photocatalysts relative to the redox potentials of compounds involved in CO_2 reduction at pH 7.[8]

However the proton assisted multiple electron reduction of CO_2 is quit easier process. The products of the multi-electron reduction of carbon dioxide are formic acid, carbon monoxide, formaldehyde, methanol, methane etc.

$CO_2 + 2e^- + 2H^+ \rightarrow HCOOH$	$E^0_{red} = -0.61$ V vs. SHE
$CO_2 + 2e^- + 2H^+ \rightarrow CO + H_2O$	$E^0_{red} = -0.52$ V vs. SHE
$2CO_2 + 2e^- \rightarrow CO + CO_3^{2-}$	$E^0_{red} = -0.64$ V vs. SHE
$CO_2 + 4e^- + 4H^+ \rightarrow HCHO + H_2O$	$E^0_{red} = -0.48$ V vs. SHE
$CO_2 + 6e^- + 6H^+ \rightarrow CH_3OH + H_2O$	$E^0_{red} = -0.38$ V vs. SHE
$CO_2 + 8e^- + 8H^+ \rightarrow CH_4 + 2H_2O$	$E^0_{red} = -0.24$ V vs. SHE

The adsorption of CO_2 on a semiconductor surface offers one way of activating the otherwise inert molecule for reduction. It is understood that adsorption leads to the formation of a partially charged species $CO_2^{\delta-}$ through interactions with surface atoms.[6] This adsorbate no longer has the linear symmetry of the free CO_2 molecule and thus has a lower barrier for accepting an electron because the LUMO level of CO_2 decreases as the molecule bends. Due presence of the band gap—void energy interval between the valence band (VB) and the conduction band (CB) of the order of visible light, semiconductors are an attractive type of materials for light-harvesting applications.[9] The semiconductor absorbs a photon of visible light of energy equal to or higher than that of its band gap. Due to this reason an electron gets excited from the VB into the CB, thereby leaving behind an empty state that constitutes a quasiparticle, referred to as a hole. Thus the concentration of the charge carriers, i.e. the electrons and the holes is higher in the illuminated semiconductor than that at equilibrium. After separation the charge carriers may migrate to the surface of the photocatalysts and consecutively get transferred to the adsorbed acceptor molecules. This initiates the corresponding oxidation or reduction process.[10] The actual reaction sites may be located either directly on the surface of

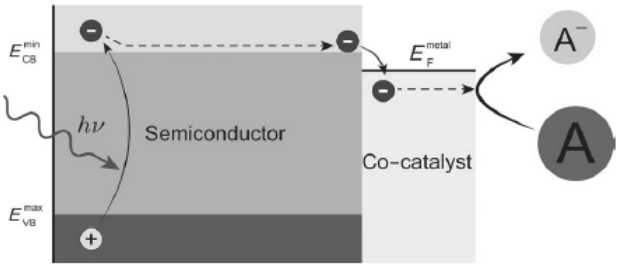

Figure 2: Schematic diagram for photogenerated electron transfer from semiconductor to the acceptor molecule via the metal co-catalyst.

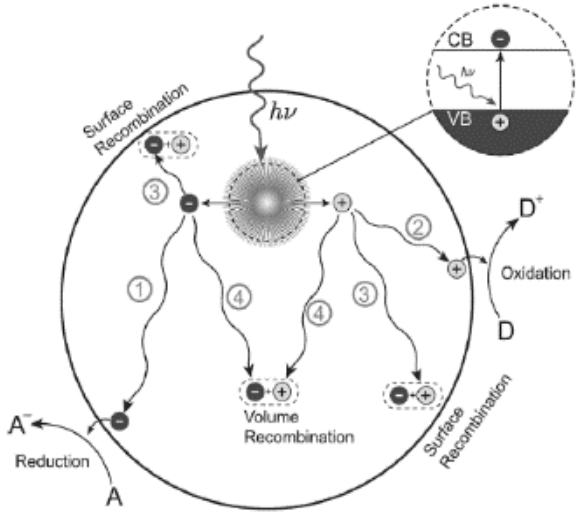

Figure 3: Schematic diagram for the photo induced formation of the electron-hole pair and the probable paths for their recombination.

the semiconductor within which the photo-excitation took place, or indirectly across the interface at the surface of another semiconductor or metal nanoparticle, which is usually referred to as the co-catalyst.[11] The primary role of the semiconductor in photocatalysis is to absorb an incident photon, generate an electron–hole pair, and facilitate its separation and transport, whereas catalysis of the reaction is an additional function which is usually performed by a different material. To get the desired redox reaction effective transfer of the charge carriers to the acceptor molecules from the semiconductor surface is required which has to compete with various recombination processes of the charge carriers. The recombination can occur by the combination of the charge carriers with their counterparts of opposite charge trapped at the semiconductor surface or at the bulk of the surface. Recombination processes decreases the efficiency of the photocatalytic systems. The back transfer of the charge carriers from the adsorbed acceptor molecules to the semiconductor surface also decreases the efficiency of a photocatalytic system.[12] The reaction conditions are typically expressed in terms of the position of the band edges: for reduction processes, the conduction band edge must lie above the lowest unoccupied molecular orbital (LUMO) of the acceptor molecule. Analogously, the transfer of a photogenerated hole from the semiconductor to an adsorbed molecule, equivalent to the transfer of an electron in the opposite direction, requires the energy level of the highest occupied molecular orbital (HOMO) of the oxidized molecule to lie above the valence band. These thermodynamic considerations mean that the choice of a suitable photocatalyst needs to be a compromise between two opposing aspects. On one hand, for reasons of efficiency, it is highly beneficial to absorb light in the visible range. This condition requires the semiconductor to have a comparably small band gap. On the other hand, as discussed above, the band gap has to span the range of the reduction and oxidation potentials relevant to the photocatalyzed reaction. The TiO_2 band structure has several specific implications for the photocatalytic reduction of CO_2. Perhaps most importantly, the single-electron reduction potential of CO_2 to the radical anion $CO_2^{\bullet-}$ at −1.9 V versus the NHE is much more negative than the conduction band of TiO_2, so that a direct electron transfer from TiO_2 to CO_2 is thermodynamically prohibited. The reduction process may proceed only through adsorbed CO_2 species on TiO_2 [13-15] or on selected metal catalysts, [16, 17] and even then the overpotential is very low.[18] Proton reduction is more favorable and, therefore, competes with CO_2 for electrons. To avoid decreasing the efficiency, the catalyst would have to suppress the H_2 generation process. It is observed that the multi-electron reduction of CO_2 to formic acid, methanol, or methane is less negative than the conduction band of TiO_2. [8] A very large number of photocatalytic systems are reported in the literature for the photocatalytic reduction of CO_2 into selected products. Mizuno and coworkers reported that illumination of suspended TiO_2 in supercritical liquid CO_2 results in the formation of $CO_2^{\bullet-}$ radicals.[19, 20] TiO_2 microcrystals embedded in SiO_2 matrices (Q-TiO_2/SiO_2) were shown to exhibit improved photocatalytic properties compared to bulk TiO_2/SiO_2 powders. These composites were dispersed in water mixed with propan-2-ol as a hole scavenger. The added CO_2 was photocatalytically converted into formate, methane, and ethene. A decrease in the Ti/Si ratio led to an increase in the efficiency of the product formation. The improved efficiency of the TiO_2/SiO_2 systems was attributed to enhanced charge separation through the presence of bridging

Ti-O-Si bonds.[21, 22] Ammonia and urea appeared in the products, together with formate and CO, when lithium nitrate was present in the solution.[23] A composite system of TiO_2 and kaolinite was examined for the photoreduction of CO_2 by Koc et al. and compared with pure P-25 TiO_2 particles in an aqueous solution of 0.2M NaOH under UV illumination.[24] The rates of formation of methane and methanol increased, but the rate of formation of CO, although generally small, was smaller for the TiO_2/kaolinite system than for P-25. Various factors were proposed to explain the enhanced performance of the composite photocatalyst. These include a larger effective surface area because of a weaker agglomeration of the particles, a reduced recombination rate of the photogenerated charges, a modified acidity of the surface of the composite system, and a smaller size of the anatase crystallites. In a study focused on finding photocatalysts able to form C_2 and possibly C_3 compounds from CO_2, TiO_2 catalysts were supported on amphiphilic materials. The dependence of the selectivity for specific photocatalytic products on the nature of the catalytic support shows its importance for the process. The highest yields and best selectivity was obtained for a 10 wt%TiO_2/Pd/Al_2O_3 system, which produced acetone and ethanol as major products, and ethane and methane as minor products from a CO_2-saturated aqueous solution.[25] In another study, a two-way approach was chosen to improve the photocatalytic activity of TiO_2 by dispersing TiO_2 nanocrystallites in the channels of a mesoporous silicate (SBA-15) and loading this composite structure with copper. Irradiation of the photocatalyst in an aqueous solution of 0.1N NaOH saturated with CO_2 led to the formation of methanol. The highest photocatalytic activity was observed for a structure of highly dispersed anatase NPs loaded with 2 wt% Cu embedded in SBA-15. The superior performance was attributed to the highly dispersed state of TiO_2 because of the mesoporous structure of SBA-15, on the one hand, and to the catalytic properties of copper, on the other hand [26]. Copper is particularly appealing compared to other metals such as platinum, rhodium, palladium, gold, and ruthenium because it is inexpensive and abundant. However, all of these metals are known for their outstanding catalytic properties. In an early study by Ishitani et al., palladium led to the largest increase in the rate of formation of methane when P-25 particles were loaded with 2 wt% of the metals. Other reported products included ethene, formic acid, acetic acid, and traces of methanol.[27] Other semiconductors such as CdS,[28] ZnS,[29] MnS,[30] Bi_2S_3/CdS,[31] WO_3,[32] $SrTiO_3$,[33] $BaTiO_3$,[34] $InNbO_4$,[35] graphitic carbon nitrides[36] etc. are used as photocatalysts in the selective photocatalytic reduction of CO_2 to different products.

Hydrogen is considered to be one of the best possible alternative energy carriers.[37, 38] However, the main challenges in developing hydrogen energy are its generation and storage. Hydrogen generation from water through photocatalytic water splitting using solar energy is an ideal way that does not evolve any harmful byproducts.[39, 40] Following the development of the photo-electrochemical cell by Fujishima and Honda[41] using a semiconductor anode and a metal cathode, varieties of semiconductor based photocatalysts have been investigated for making an efficient catalyst to generate hydrogen from water. The mechanism of photocatalytic water splitting using semiconductor materials involves different steps, namely, generation of charge carriers (electron and holes) on light absorption, separation and diffusion of the photogenerated charge carriers to the active sites on the catalyst surface and further reaction (oxidation/reduction)

with the adsorbed water to generate hydrogen and oxygen.[40] Among the semiconductor based photocatalysts, TiO_2 has been extensively investigated due to its potential to split water. However, its wide bandgap (~3.0 eV) limits its activity to the UV region of the solar spectrum.[42] During the past few years, extensive efforts have been dedicated to enhance the visible light activity of TiO2, mainly by doping with different metal or nonmetal elements.[42] Apart from TiO2, many other transition metal oxides, sulfides, and selenides, such as ZnO, $SrTiO_3$, $NaTaO_3$, ZnS, CdS, CdSe, etc., have been studied for photocatalytic water splitting.[42-48] Other than these conventional materials, polymeric semiconductor materials like graphitic carbon nitrides are also found to have great potential as photocatalyst. Wang et al.[49] have reported the melem-based graphitic carbon nitrides (g-C_3N_4) as a metal-free photocatalyst for visible-light driven water splitting. However, this material is reported to show very poor quantum yield, which is attributed to the high recombination rate of the photogenerated electron−hole pairs. To overcome this problem, many attempts have been made to tune the properties, namely, doping, metal decoration, introducing porosity, making graphene/g-C_3N_4 composites, etc.[50-53] Pan et al.[54] have shown that the g-C_3N_4 nanotubes have better carrier mobilities in comparison with the 2D sheets, and further enhancement in photocatalytic activity upon functionalization of these tubes with metals like Pt and Pd is reported. Wang et al.[55] have observed enhanced photocatalytic activity for nanocomposites made of g-C_3N_4 and MoS_2 in comparison to pure g-C_3N_4. Very recently, Shi et al.[56] have synthesized composites of mesoporous carbon and g-C_3N_4 and observed significant improvement in photocatalytic activity. Apart from the g-C_3N_4, another polymeric carbon nitride, the poly(triazine imide), is also found to be a potential photocatalyst for water splitting.[57-59]

In the chemical reduction, carbon dioxide is hydrogenated in presence metal complexes as catalysts. Conversion of CO_2 into useful organic products is the key step as carbon dioxide is an important feedstock for organic chemicals due to its low cost, high abundance, and lower toxicity. Reduction of CO_2 to CO is a crucial step for methanol synthesis and the hydroformylation reaction.[60-63] There are two advantages of using metal-complex based electrocatalysts over others. First, metal complexes can be tuned easily by ligand modifications. Second, metal complexes can have a vacant site available initially or during the course of the reaction.[64] Various transition metal-based complexes (Ni, Fe, Re, Cr, Ir, Mo, etc.) have been studied extensively for the homogeneous electrocatalytic reduction of carbon dioxide.[65-71] Direct reduction of CO_2 in aprotic solvent at inert electrodes, by applying negative potential close to the standard potential of the $CO_2/CO_2^{\bullet-}$ redox couple (−2.21 V vs. SCE in DMF + 0.1 M Bu_4NClO_4), yields oxalate in good proportion. This process involves a nucleophilic addition of the catalyst radical anion on CO_2 forming an oxygen−carbon bond, which further breaks homolytically, generating the parent ester and $CO_2^{\bullet-}$, which would then dimerize to produce oxalate. A similar process occurred when using electrogenerated macrocyclic Ni(I) chelate complexes, leading, upon electrolysis at a potential close to −2.15 V vs. SCE in an acetonitrile solution saturated with CO_2, to oxalate production with faradaic yield equal or larger than 90% and a maximum TON of 750. In that case, the electrode was a mercury pool, and the counter electrode (not separated from the cathodic compartment) was an aluminum wire.[72] Recently a striking study for CO_2 to oxalate transformation is published in

which a binuclear Cu complex to both capture and reduce CO_2 from the air to produce oxalate in quantitative yield at very low overpotential at a glassy carbon electrode (TON = 6).[73] Eisenberg et al.[74] and Sauvage et al.[65, 75] pioneered the use of Ni macrocycle complexes to reduce CO_2 into CO. The $Ni(cyclam)^{2+}$ complex converts CO_2 to CO very efficiently and selectively (high TON and high FE) in water (pH 4 to 5) and in an aprotic solvent (DMF) under 1 atm CO_2 led to production of formic acid mainly with 75% faradaic efficiency and a TON of 3.2 (and 15% of CO).[76] A representative example concerns the use of tetraazamacrocycle, that was first investigated by Tinnemans et al.[77] and Che. et al.[78] in the 1980s. For example, Che et al. have shown that electrolysis in acetonitrile at a carbon electrode produces CO in 20−30% faradaic yield. Another example of an efficient Co catalyst for the CO_2 to CO conversion was discovered with a macrocycle including four aminopyridine as ligands, linked by pendant amine groups. Highly selective CO formation (98%) could be sustained for a couple of hours in a DMF solution saturated with CO_2 and containing 1.2M of trifluoroethanol as a weak acid to help the catalysis.[79] A new class of highly active Mn catalysts was introduced by Chardon-Noblat and Deronzier et al. They used $Mn(L)(CO)_3Br$ complexes with L being either a 2,2′- bipyridine or a 4,4′-dimethyl-2,2′-bipyridine ligand.[80, 81] A 4 h electrolysis with L = 2,2′- bipyridine in CH_3CN (ACN) + 5% H_2O at −1.40 versus SCE (420 mV overpotential) and 0.2 mA/cm^2 converts CO_2 into CO with unity faradaic efficiency. In the search of new catalysts, Mn(I) complexes with a planar coordinating tridentate PNP ligand and bearing a positive charge was recently synthesized and studied, showing excellent efficiency for CO production (close to 100%) in dry acetonitrile.[82] Very recently Rawat et al. reported that A bifunctional, chelating N-heterocyclic carbene-pyridine (NHC-pyridine) containing Mn(I) complex [MnBr(NHC-pyridine)$(CO)_3$] displays a strong selectivity for CO_2 reduction over proton reduction to generate CO.[83] Iron porphyrins, when electrochemically reduced to the Fe(0) species, are among the most efficient molecular catalysts for the CO_2 to CO conversion in aprotic solvent (DMF, ACN), in terms of both efficiency, catalytic rate and robustness.[84-87] Recently Rawat et al. reported that the Fe complex $[Cp^{C6F5}Fe(P^{tBu}{}_2N^{tBu}{}_2)]^+$ containing the electron-withdrawing CpC_6F_5 ligand is the most active catalyst to convert CO_2 to $HCOO^-$ with a total free energy barrier of only 14.9 kcal/mol. Besides, they found that the rate determining steps (heterolytic cleavage and hydride transfer) of CO_2 hydrogenation are improved significantly when catalyzed by the pendant amine based $[Cp^{C6F5}Fe(P^{tBu}{}_2N^{tBu}{}_2)]^+$ complex.[88]

Thus it requires a vast theoretical investigation and knowledge to explain and characterize the mechanisms of such catalytic and photocatalytic reactions and predict newer and efficient catalytic and photocatalytic surfaces and metal complexes for the activation of such molecules to produce valuable chemicals.

The solution processability and tunable electronic structure of conjugated organic molecules like poly-thiophenes, poly-acenes and heteroacenes, etc. make them attractive for use in different optoelectronic devices.[89, 90] The tunability of the electronic structure of such molecules arises from their susceptibility towards different functionalization at the aromatic ring. Thus, by the advent of the sophisticated organic synthetic methodologies one can use them as per the requirement in molecular electronics. Semiconducting organic molecules can be classified as hole

transporter and electron transporter depending on their role in the composite electronic junction. More precisely, if they induce p-type of effect, they are hole conducting and if they induce n-type of effect, they are electron transporting material. Most of the known organic electronics are of p-type as because those materials are more stable in ambient condition and their reported carrier mobilities are higher in comparison to that of n-type materials.[90, 91] Nevertheless, stable n-type organic semiconductors are also of complementary interest to prepare p-n junction and other logic circuits and thus are now evolving.[92] Unusual n-type organic semiconductors have recently been realized by introducing electron withdrawing groups to the thiophene or acene oligomers which are originally known as hole-transporting materials. Stereo-electronic effects have also been attributed for such kind of carrier switching in a different kind of materials.[93] In the molecular level, by incorporation of an electron-withdrawing group or by conformational change it lowers the energy level of lowest unoccupied molecular orbital (LUMO) which provokes the overcoming the energy barrier for electron conduction.[94, 95] The major cause behind the unavailability of high performance n-type organic semiconductors is the scarcity of suitable electron withdrawing groups that can stabilize the semiconductor materials with desired electron transport characteristics.[96] The electron injection into the LUMO of the organic semiconductor is equivalent to a reduction process in an electrochemical reaction. Now, if the above mentioned LUMO is of relatively high energetic, the injected electron is prone to react with some species such as aerial O2 and H2O in ambient condition and thus the electron transport is annihilated. It has been established, both theoretically and empirically, that for obtaining a stable electron transporting organic semiconductor, the LUMO energy of the material should lie at around -4 eV.[96] The lower LUMO energy on the other hand reduces the electron injection barrier height which is defined as the energy difference between the semiconductor-LUMO and the Fermi energy (EF) of the source electrode, such as Au (111) surface. So, identifying an organic semiconductor as 'p-type' or 'n-type' is of fundamental interest and analyzing their transport characteristics and making way out their inter-conversion is really demanding in the field of organic electronics. Furthermore, identification of the crossover point at which the carrier switching is occurred is very challenging. However, to characterize the carrier type one has to design proper molecular contact, as because molecular conductance depends on the intra and intermolecular coupling scheme.[97] Modern sophisticated techniques such as scanning tunneling microscopy (STM), atomic force microscopy (AFM) along with the molecular break junction (BJ) method, however, have been successfully utilized to fabricate metal-molecule-metal contact through selective site attachment.[98] In STM-BJ technique, a molecule is bridged in between two nanoscale gold electrodes and its conductance is measured. The conductance depends on the energetic alignment of the frontier molecular orbitals with the Fermi level of the metal (in most cases, gold) electrodes. It is worth mentioning that, the molecular transport is characterized as "electron transport" ("hole transport") if the conduction is mediated by tunneling through the LUMO (HOMO).[99] Thus, it requires a deep theoretical understanding on the electronic structure of the molecule and the metal-molecule contact to characterize the nature of charge carrier.

Objectives of our proposed research work

(1) We would try to computationally design efficient catalytic and photo-catalytic systems for activation CO_2, water and other molecules to produce environmentally sustainable and benign sources of energy and study the mechanisms of the reactions.

(2) We are now studying the electronic properties of carbon-nitride based nanomaterials to observe their effectiveness towards catalytic and photo-catalytic activation of CO_2, water and other molecules.

Our objective is to introduce defects and doping into the intrinsic carbon-nitride based nanomaterial and modify their electronic properties to enhance the rate of charge transfer for the activation of CO_2, water and other molecules to generate sustainable sources of energy.

(3) We are also studying the transport phenomenon through the single-molecule junction based on S,N-hetroacenes. These junctions exhibit carrier switching on modification of the junction backbone. Our goal in this area is to search for better junction structure for the efficient transport of the charge carriers.

Methodology

Assuming nuclei and electrons as point masses and neglecting spin-orbit and other relativistic interactions the Hamiltonian operator for a cluster of atoms or a molecule is given by,

$$\hat{H} = -\frac{\hbar^2}{2}\sum_{\alpha}\frac{1}{m_\alpha}\nabla_\alpha^2 - \frac{\hbar^2}{2m_e}\sum_{i}\nabla_i^2 + \sum_{\alpha}\sum_{\beta>\alpha}\frac{Z_\alpha Z_\beta e'^2}{r_{\alpha\beta}} - \sum_{\alpha}\sum_{i}\frac{Z_\alpha e'^2}{r_{i\alpha}} + \sum_{j}\sum_{i>j}\frac{e'^2}{r_{ij}}$$

Kinetic energy operator for nuclei | Kinetic energy operator for electrons | Nuclei-nuclei repulsion term | Nuclei-electron attraction term | Electron-electron repulsion term

where α, β refer to nuclei and i, j refer to electrons and

m_α= Mass of nucleus α;

m_e= Mass of an electron;

Z_α= Atomic number of nucleus α;

$r_{\alpha\beta}$= Distance between nuclei α and β;

$r_{i\alpha}$= Distance between electron I and nucleus α;

r_{ij}= Distance between electrons i and j;

and $e'^2 = \frac{e^2}{4\pi\varepsilon_0}$, where e is the charge of an electron.

Since nuclei are much heavier than electrons, the electrons move much faster than the nuclei. Hence according to ***Born-Oppenheimer approximation***, we can regard the nuclei as fixed while the electrons carry out their motions. Thus considering the nuclei as fixed operator for the nuclear kinetic energy is omitted from the above equation and considering the nuclei-nuclei repulsion term (V_{NN}) as constant, the Schrödinger equation for electronic motion is given by,

$$(\hat{H}_{el} + V_{NN})\psi_{el} = U\psi_{el}$$

where the purely electronic Hamiltonian operator $\hat{H}_{el}$ is given by,

$$\hat{H}_{\text{el}} = -\frac{\hbar^2}{2m_e}\sum_i \nabla_i^2 - \sum_\alpha \sum_i \frac{Z_\alpha e'^2}{r_{i\alpha}} + \sum_j \sum_{i>j} \frac{e'^2}{r_{ij}}$$

and the energy U = electronic energy including internuclear repulsion energy. The internuclear distances ($r_{\alpha\beta}$) in the molecular Hamiltonian operator are not variables but, are each fixed at some constant value. There are infinite number of possible nuclear configurations, and for each of these we may solve the electronic Schrödinger equation to get a set of electronic wave functions and corresponding electronic energies. Each member of the set corresponds to a different molecular electronic state. The electronic wave functions and energies thus parametrically depend on the nuclear coordinates (q_α) as,

$$\psi_{el} \equiv \psi_{el,n}(q_i; q_\alpha) \qquad \text{and} \qquad U \equiv U(q_\alpha)$$

where, n symbolizes the electronic quantum numbers.

The variables in the electronic Schrödinger equation are electronic coordinates (q_i) and the quantity V_{NN} is independent of these coordinates and it is constant for a particular nuclear configuration. Hence omitting the constant term (V_{NN}) from the Hamiltonian the Schrödinger equation for pure electronic motion is given by,

$$\hat{H}_{el}\psi_{el} = E_{el}\psi_{el}$$

where, purely electronic energy (E_{el}) is related to the electronic energy including internuclear repulsion (V_{NN}) by

$$U = E_{el} + V_{NN}$$

Thus determining the purely electronic energy (E_{el}) by solving the purely electronic Schrödinger equation by ***Density Functional Theory*** method and adding V_{NN} to E_{el} the total electronic energy (U) of a system can be obtained.

Future Prospect

(1) We will study the catalytic and photocatalytic properties of different isolated graphitic carbon nitride based systems and other semiconductor surfaces by means of Density Functional theory based calculations.

(2) We will study the application of different composite systems (such as Al-cluster & graphitic carbon nitride composite and others) on the catalytic and photocatalytic activation of small molecules such as CO_2, H_2O, N_2, etc. to produce valuable chemicals necessary in our daily life.

(3) We will study the physical accounts of the transport characteristics of different molecular junctions and try to explore the nature of charge carriers dictated by the change of junction backbone based on abinitio quantum mechanical studies.

References

1. e. W. Ayers, American Chemical Society, Washington, D.C., 1988.
2. R. L. House, N. Y. M. Iha, R. L. Coppo, L. Alibabaei, B. D. Sherman, P. Kang, M. K. Brennaman, P. G. Hoertz and T. J. Meyer, *J. Photochem. Photobiol., C*, 2015, **25**, 32.
3. D. Kim, K. K. Sakimoto, D. Hong and P. Yang, *Angew. Chem., Int. Ed.*, 2015, **54**, 3259.
4. A. Taheri and L. A. Berben, *Chem. Commun.*, 2016, **52**, 1768.
5. H. J. Freund and M. W. Roberts, *Surf. Sci. Rep.*, 1996, **25**, 225-273.
6. V. P. Indrakanti, J. D. Kubicki and H. H. Schobert, *Energy Environ. Sci.*, 2009, **2**, 745-758.
7. W. H. Koppenol and J. D. Rush, *J. Phys. Chem.*, 1987, **91**, 4429-4430.
8. P. D. Tran, L. H. Wong, J. Barber and J. S. C. Loo, *Energy Environ. Sci.*, 2012, **5**, 5902-5918.
9. M. R. Hoffmann, S. T. Martin, W. Choi and D. W. Bahnemann, *Chem. Rev.*, 1995, **95**, 69-96.
10. A. L. Linsebigler, G. Lu and J. T. Yates, *Chem. Rev.*, 1995, **95**, 735-758.
11. P. V. Kamat, *J. Phys. Chem. Lett.*, 2012, **3**, 663-672.
12. S. Habisreutinger, L. Schmidt-Mende and J. Stolarczyk, *Angew. Chem. Int. Ed.*, 2013, **52**, 7372-7408.
13. J. Lee, D. C. Sorescu and X. Deng, *J. Am. Chem. Soc.*, 2011, **133**, 10066-10069.
14. S. Tan, Y. Zhao, J. Zhao, Z. Wang, C. Ma, A. Zhao, B.Wang, Y. Luo, J. Yang and J. Hou, *Phys. Rev. B*, 2011, **84**, 155418.
15. A. G. Thomas and K. L. Syres, *Chem. Soc. Rev.*, 2012, **41**, 4207-4217.
16. J. Rasko and F. Solymosi, *J. Phys. Chem.*, 1994, **98**, 7147-7152.
17. A. A. Peterson, F. Abild-Pedersen, F. Studt, J. Rossmeisl and J. K. Norskov, *Energy Environ. Sci.*, 2010, **3**, 1311-1315.
18. A. A. Peterson and J. K. Nørskov, *J. Phys. Chem. Lett.*, 2012, **3**, 251-258.

19. S. Kaneco, H. Kurimoto, K. Ohta, T. Mizuno and A. Saji, *J. Photochem. Photobiol. A*, 1997, **109**, 59-63.
20. S. Kaneco, H. Kurimoto, Y. Shimizu, K. Ohta and T. Mizuno, *Energy*, 1999, **24**, 21-30.
21. H. Inoue, T. Matsuyama, B. J. Liu, T. Sakata, H. Mori and H. Yoneyama, *Chem. Lett.*, 1994, **23**, 653-656.
22. B. J. Liu, T. Torimoto, H. Matsumoto and H. Yoneyama, *J. Photochem. Photobiol. A*, 1997, **108**, 187-192.
23. B. J. Liu, T. Torimoto and H. Yoneyama, *J. Photochem. Photobiol. A*, 1998, **115**, 227-230.
24. K. Kocl, V. Matejka, P. Kovar, Z. Lacny and L. Obalova, *Catal. Today*, 2011, **161**, 105-109.
25. M. Subrahmanyam, S. Kaneco and N. Alonso-Vante, *Appl. Catal. B*, 1999, **23**, 169-174.
26. H. C. Yang, H. Y. Lin, Y. S. Chien, J. Wu and H. H. Wu, *Catal. Lett.*, 2009, **131**, 381-387.
27. O. Ishitani, C. Inoue, Y. Suzuki and T. Ibusuki, *J. Photochem. Photobiol. A*, 1993, **72**, 269-271.
28. P. Johne and H. Kisch, *J. Photochem. Photobiol. A*, 1997, **111**, 223-228.
29. H. Fujiwara, H. Hosokawa, K. Murakoshi, Y. Wada, S. Yanagida, T. Okada and H. Kobayashi, *J. Phys. Chem. B*, 1997, **101**, 8270-8278.
30. X. V. Zhang, S. T. Martin, C. M. Friend, M. A. A. Schoonen and H. D. Holland, *J. Am. Chem. Soc.*, 2004, **126**, 11247-11253.
31. X. Li, J. Chen, H. Li, J. Li, Y. Xu, Y. Liu and J. Zhou, *J. Nat. Gas Chem.*, 2011, **20**, 413-417.
32. Y. P. Xie, G. Liu, L. Yin and H. M. Cheng, *J. Mater. Chem.*, 2012, **22**, 6746-6751.
33. J. C. Hemminger, R. Carr and G. A. Somorjai, *Chem. Phys. Lett.*, 1978, **57**, 100-104.
34. B. R. Eggins, P. K. J. Robertson, E. P. Murphy, E. Woods and J. T. S. Irvine, *J. Photochem. Photobiol. A*, 1998, **118**, 31-40.
35. D. S. Lee, H. J. Chen and Y. W. Chen, *J. Phys. Chem. Solids*, 2012, **73**, 661-669.
36. G. Gao, Y. Jiao, E. R. Waclawik and A. Du, *J. Am. Chem. Soc.*, 2016, **138**, 6292-6297.
37. N. S. Lewis and D. G. Nocera, *Proc. Natl. Acad. Sci. U.S.A.*, 2006, **103**, 15729−15735.
38. A. Züttel, A. Remhof, A. Borgschulte and O. Friedrichs, *Philos. Trans. R. Soc., A*, 2010, **368**, 3329-3342.
39. A. J. Bard and M. A. Fox, *Acc. Chem. Res.*, 1995, **28**, 141-145.
40. R. M. N. Yerga, M. C. A. Galván, F. del Valle, J. A. V. de la Mano and J. L. G. Fierro, *ChemSusChem*, 2009, **2**, 471-485.
41. A. Fujishima and K. Honda, *Nature*, 1972, **238**, 37-38.
42. K. Hashimoto, H. Irie and F. A., *Jpn. J. Appl. Phys. Part*, 2005, **44**, 8279-8285.
43. K. Maeda and K. Domen, *J. Phys. Chem. C*, 2007, **111**, 7851-7861.
44. A. Kudo and Y. Miseki, *Chem. Soc. Rev.*, 2009, **38**, 253-278.
45. X. Chen, S. Shen, L. Guo and S. S. Mao, *Chem. Rev.*, 2010, **110**, 6503-6570.
46. K. Maeda and K. Domen, *J. Phys. Chem. Lett.*, 2010, **1**, 2655-2661.
47. P. Liu, J. Nisar, R. Ahuja and B. Pathak, *J. Phys. Chem. C*, 2013, **117**, 5043-5050.
48. B. Modak, K. Srinivasu and S. K. Ghosh, *J. Phys. Chem. C*, 2014, **118**, 10711-10719.
49. X. Wang, K. Maeda, A. Thomas, K. Takanabe, G. Xin, J. M. Carlsson, K. Domen and M. Antonietti, *Nat. Mater.*, 2008, **8**, 76-80.
50. J. Zhang, X. Chen, K. Takanabe, K. Maeda, K. Domen, J. D. Epping, X. Fu, M. Antonietti and X. Wang, *Angew. Chem., Int. Ed.*, 2010, **49**, 441-444.
51. Y. Zhang, T. Mori, L. Niu and J. Ye, *Energy Environ. Sci.*, 2011, **4**, 4517-4521.
52. X. Ma, Y. Lv, J. Xu, Y. Liu, R. Zhang and Y. Zhu, *J. Phys. Chem. C*, 2012, **116**, 23485-23493.
53. Y. Zheng, J. Liu, J. Liang, M. Jaroniec and S. Z. Qiao, *Energy Environ. Sci.*, 2012, **5**, 6717-6731.
54. H. Pan, Y. W. Zhang, V. B. Shenoy and H. Gao, *ACS Catal.*, 2011, **1**, 99-104.
55. J. Wang, Z. Guan, J. Huang, Q. Li and J. Yang, *J. Mater. Chem. A*, 2014, **2**, 7960-7966.
56. L. Shi, L. Liang, J. Ma, F. Wang and J. Sun, *Dalton Trans.*, 2014, **43**, 7236.

57. E. J. McDermott, E. Wirnhier, W. Schnick, K. S. Virdi, C. Scheu, Y. Kauffmann, W. D. Kaplan, E. Z. Kurmaev and A. Moewes, *J. Phys. Chem. C*, 2013, **117**, 8806-8812.
58. K. Schwinghammer, B. Tuffy, M. B. Mesch, E. Wirnhier, C. Martineau, F. Taulelle, W. Schnick, J. Senker and B. V. Lotsch, *Angew. Chem., Int. Ed.*, 2013, **52**, 2435-2439.
59. K. Schwinghammer, M. B. Mesch, V. Duppel, C. Ziegler, J. Senker and B. V. Lotsch, *J. Am. Chem. Soc.*, 2014, **136**, 1730-1733.
60. J. P. Lange, *Catal. Today*, 2001, **64**, 3-8.
61. O. Martin and J. Perez-Ramirez, *Catal. Sci. Technol.*, 2013, **3**, 3343-3352.
62. J. Frenzel, J. Kiss, N. N. Nair, B. Meyer and D. Marx, *Phys. Status Solidi B*, 2013, **250**, 1174-1190.
63. E. S. Wiedner and A. M. Appel, *J. Am. Chem. Soc.*, 2014, **136**, 8661-8668.
64. M. D. Doherty, D. C. Grills, J. T. Muckerman, D. Polyansky and E. Fujita, *Coord. Chem. Rev.*, 2010, **254**, 2472-2482.
65. M. Beley, J. Collin, R. Ruppert and J. P. Sauvage, *J. Am. Chem. Soc.*, 1986, **108**, 7461-7467.
66. E. Fujita, J. Haff, R. Sanzenbacher and H. Elias, *Inorg. Chem.*, 1994, **33**, 4627-4628.
67. M. L. Clark, K. A. Grice, C. E. Moore, A. L. Rheingold and C. P. Kubiak, *Chem. Sci.*, 2014, **5**, 1894-1900.
68. C. He, G. Tian, Z. Liu and S. A. Feng, *Org. Lett.*, 2010, **12**, 649-651.
69. P. Kang, C. Cheng, Z. Chen, C. K. Schauer, T. Meyer and M. Brookhart, *J. Am. Chem. Soc.*, 2012, **134**, 5500-5503.
70. E. Portenkirchner, Kianfar, N. S. Sariciftci and G. Knör, *ChemSusChem*, 2014, **7**, 1347-1351.
71. J. Song, E. L. Klein, F. Neese and S. Ye, *Inorg. Chem.*, 2014, **53**, 7500-7507.
72. M. Rudolph, S. Dautz and E. G. Jäger, *J. Am. Chem. Soc.*, 2000, **122**, 10821-10830.
73. R. Angamuthu, P. Byers, M. Lutz, A. L. Spec and E. Bouwman, *Science*, 2010, **327**, 313-315.
74. B. Fisher and R. Eisenberg, *J. Am. Chem. Soc.*, 1980, **102**, 7361-7363.
75. M. Beley, J. P. Collin, R. Ruppert and J. P. Sauvage, *Chem. Commun.*, 1984, **2**, 1315-1316.
76. J. P. Collin, A. Jouaiti and J. P. Sauvage, *Inorg. Chem.*, 1988, **27**, 1986-1990.
77. A. H. A. Tinnemans, T. P. M. Koster, D. H. M. W. Thewissen and A. Mackor, *Recl. Trav. Chim. Pays-Bas*, 1984, **103**, 288-295.
78. C. M. Che, S. T. Mak, W. O. Lee, K. W. Fung and T. C. W. Mak, *J. Chem. Soc. Dalton Trans.*, 1988, 2153-2159.
79. A. Chapovetsky, T. A. Do, R. Haiges, M. K. Takase and S. C. Marinescu, *J. Am. Chem. Soc.*, 2016, **138**, 5765-5768.
80. M. Bourrez, F. Molton, S. Chardon-Noblat and A. Deronzier, *Angew. Chem. Int. Ed.*, 2011, **50**, 9903-9906.
81. M. Bourrez, M. Orio, F. Molton, H. Vezin, C. Duboc, A. Deronzier and S. Chardon-Noblat, *Angew. Chem. Int. Ed.*, 2014, **53**, 240-243.
82. G. K. Rao, W. Pell, I. Korobkov and D. Richeson, *Chem. Commun.*, 2016, **52**, 8010-8013.
83. K. S. Rawat, A. Mahata, I. Choudhuri and B. Pathak, *J. Phys. Chem. C*, 2016, **120**, 8821-8831.
84. C. Costentin, S. Drouet, M. Robert and J. M. Savéant, *Science*, 2012, **338**, 90-94.
85. J. M. Savéant, *Chem. Rev.*, 2008, **108**, 2348-2378.
86. C. Costentin, M. Robert and J. M. Savéant, *Chem. Soc. Rev.*, 2013, **42**, 2423-2436.
87. C. Costentin, M. Robert and J. M. Savéant, *Acc. Chem. Res.*, 2015, **48**, 2996-3006.
88. K. S. Rawat, A. Mahata and B. Pathak, *J. Phys. Chem. C*, 2016, **120**, 26652-26662.
89. C. Wang, H. Dong, W. Hu, Y. Liu and D. Zhu, *Chem. Rev.*, 2011, **112**, 2208–2267.
90. C.-H. Tsai, D. N. Chirdon, A. B. Maurer, S. Bernhard and K. J. Noonan, *Org. Lett.*, 2013, **15**, 5230-5233.
91. I. Osaka, R. Zhang, G. Sauvé, D.-M. Smilgies, T. Kowalewski and R. D. McCullough, *J. Am. Chem. Soc.*, 2009, **131**, 2521–2529.

92. J. E. Cochran, E. Amir, K. Sivanandan, S.-Y. Ku, J. H. Seo, B. A. Collins, J. R. Tumbleston, M. F. Toney, H. Ade and C. J. Hawker, *J. Poly. Sci. Part B: Pol. Phy.*, 2013, **51**, 48-56.
93. T. A. Su, H. Li, M. L. Steigerwald, L. Venkataraman and C. Nuckolls, *Nat. Chem.*, 2015, **7**, 215-220.
94. B. Capozzi, J. Xia, O. Adak, E. J. Dell, Z.-F. Liu, J. C. Taylor, J. B. Neaton, L. M. Campos and L. Venkataraman, *Nat. Nanotech.*, 2015.
95. A. Pramanik and P. Sarkar, *J. Chem. Phys.*, 2015, **143**, 114314.
96. J. T. Quinn, J. Zhu, X. Li, J. Wang and Y. Li, *J. Mat. Chem. C*, 2017, **5**, 8654-8681.
97. K.-H. Müller, *Phys. Rev. B*, 2006, **73**, 045403.
98. B. Xu and N. J. Tao, *Science*, 2003, **301**, 1221-1223.
99. Y. Xue and M. A. Ratner, *Phys. Rev. B*, 2003, **68**, 115406.